

Modeling the Geochemical Impact of an Injection of CO₂ and Associated Reactive Impurities into a Saline Reservoir

Laurent André, Mohamed Azaroual, Christian Bernstone, Andrea Wittek

► **To cite this version:**

Laurent André, Mohamed Azaroual, Christian Bernstone, Andrea Wittek. Modeling the Geochemical Impact of an Injection of CO₂ and Associated Reactive Impurities into a Saline Reservoir. TOUGH Symposium 2012, Sep 2012, Berkeley, United States. 8 p. hal-00755058

HAL Id: hal-00755058

<https://hal-brgm.archives-ouvertes.fr/hal-00755058>

Submitted on 20 Nov 2012

HAL is a multi-disciplinary open access archive for the deposit and dissemination of scientific research documents, whether they are published or not. The documents may come from teaching and research institutions in France or abroad, or from public or private research centers.

L'archive ouverte pluridisciplinaire **HAL**, est destinée au dépôt et à la diffusion de documents scientifiques de niveau recherche, publiés ou non, émanant des établissements d'enseignement et de recherche français ou étrangers, des laboratoires publics ou privés.

MODELING THE GEOCHEMICAL IMPACT OF AN INJECTION OF CO₂ AND ASSOCIATED REACTIVE IMPURITIES INTO A SALINE RESERVOIR

Laurent ANDRE¹, Mohamed AZAROUAL¹, Christian BERNSTONE², Andrea WITTEK²

¹BRGM - Water, Environment and Ecotechnology Direction,
Avenue Claude Guillemin, BP 36009, F-45060 ORLEANS Cedex 2 - France

²VATTENFALL, Research and Development AB, Puschkinallee 52, 12435 BERLIN – Germany
e-mail : l.andre@brgm.fr; m.azaroual@brgm.fr; christian.bernstone@vattenfall.com; andrea.wittek@vattenfall.de

ABSTRACT

Numerical simulations performed with the TOUGHREACT code focus on the chemical reactivity of deep reservoir rock impacted by an injection of CO₂ and associated reactive impurities (mainly SO₂ and O₂). A simplified two-dimensional radial geo-model representing the near wellbore domain of a saline reservoir enabled us to capture the global geochemical behaviour of this underground zone. Two ratios CO₂/SO₂ are investigated. The results of the numerical simulations highlight the high reactivity of the near-well zone in the case where ancillary gases (SO₂ and O₂) are injected with CO₂ with dissolution of carbonates and precipitation of sulfate minerals. Major reactions occur in the reservoir formation, whereas clays of the caprock are only slightly affected by the injection of CO₂ and associated reactive impurities.

INTRODUCTION

Numerical simulations using coupled hydrogeological, thermal, and geochemical codes as TOUGHREACT (Xu and Pruess, 2001) serve as adequate tools to explore different evolution scenarios of gas injection in deep geological structures, and to determine the behavior of the near-wellbore region of the targeted reservoir. Previous numerical studies have demonstrated that massive and continuous injection of pure CO₂ involves a disequilibrium of the physical characteristics (temperature, gas saturation, pressure, capillary pressure...) and geochemical characteristics (dissolution of supercritical CO₂ into the brine, pH variations, dissolution/ precipitation reactions of the porous rock minerals) of the host reservoir (André et al., 2007, 2010).

However, the presence of impurities in the CO₂ gas stream may impair the engineering processes

of capture, transport, and injection: some associated reactive gases, i.e., chemical species other than CO₂ in the injected stream—namely SO_x, NO_x, H₂S, or O₂—may require different adaptations for injection and disposal than if the stream were pure CO₂. Moreover, the presence of associated gases in the CO₂ stream in relatively high proportions can affect the compressibility of the injected gas and reduce the CO₂ storage capacity of the reservoir. This is because of the space taken up by these gases and the unfavorable volume balance of induced geochemical reactions. Additionally, depending on the type of geological storage, the presence of ancillary gases may have some other specific effects, such as trapping performances. In the case of CO₂ storage in deep saline formations, the presence of gas impurities affects the gas solubility in the aqueous phase, as well as the rate and amount of CO₂ stored through mineral dissolution and precipitation.

Hence, we need numerical estimations to forecast how the gas composition might impact the geochemical reactivity inside the host reservoir, potentially modifying the porosity and permeability of the medium and influencing the long-term well injectivity. Two numerical simulations are performed to study the impact of CO₂, SO₂ and O₂ mixtures on the main physico-chemical characteristics of a deep saline aquifer.

NUMERICAL APPROACH

Calculation code

The TOUGHREACT simulator (Xu and Pruess, 2001) is used for all simulations in this study. This code, which issued from TOUGH2 V2 (Pruess et al., 1999), couples thermal, hydraulic and chemical (THC) processes and is applicable to one-, two-, or three-dimensional geologic systems with physical and chemical heterogeneity. TOUGHREACT is coupled with

ECO2n (Pruess, 2005), a fluid property module developed specifically to deal with geologic sequestration of CO₂ in saline aquifers. It can be used to model isothermal or nonisothermal multiphase flow in water/brine/CO₂ systems.

TOUGHREACT simulates the chemical reactivity of systems based on an extended thermodynamic database. In this study, we use the database released with the program, i.e., a modified version of the EQ3/6 database (Wolery, 1992).

Thermodynamic equilibrium between the gas phase and the aqueous phase is assumed for CO₂ dissolution. An extension of Henry's law, including salting-out effect, is used to estimate the solubility of CO₂ in the aqueous phase at high pressure and high salinity.

For this work, the dissolution and precipitation reactions of minerals proceed under kinetic constraints. The general form of the rate law proposed by Lasaga (1984) is applied for both dissolution and precipitation of minerals:

$$r_n = \pm k_n A_n |1 - \Omega_n^\theta|^\eta$$

Positive values for r_n correspond to the dissolution of the mineral n (negative for precipitation), k_n represents the rate constant (mol m⁻² s⁻¹), A_n is the specific reactive surface area per kg_{H2O}, Ω_n represents the saturation index of the mineral n ($\Omega_n = Q_n/K_n$), and θ and η are empirical parameters determined from experiments, usually taken as 1.

The dependence of the rate constant k_n with temperature is calculated by means of the Arrhenius equation:

$$k_n = k_{25} \exp\left[\frac{-E_a}{R}\left(\frac{1}{T} - \frac{1}{298.15}\right)\right]$$

where E_a is the activation energy (J mol⁻¹), k_{25} the rate constant at 25°C, R is the gas constant (J mol⁻¹ K⁻¹) and T the temperature in Kelvin.

For some minerals, specifically alumino-silicates and salts, the dissolution and precipitation also depend on H⁺ (acid mechanism) and OH⁻ (alkaline mechanism) concentrations, in addition to the neutral mechanism. In this case, k_n is calculated using the following expression:

$$k_n = k_{25}^{nu} \exp\left[\frac{-E_a^{nu}}{R}\left(\frac{1}{T} - \frac{1}{298.15}\right)\right] + k_{25}^H \exp\left[\frac{-E_a^H}{R}\left(\frac{1}{T} - \frac{1}{298.15}\right)\right] a_H^{n_H} + k_{25}^{OH} \exp\left[\frac{-E_a^{OH}}{R}\left(\frac{1}{T} - \frac{1}{298.15}\right)\right] a_H^{n_{OH}}$$

Superscripts and subscripts nu , H , and OH indicate neutral, acid, and alkaline mechanisms, respectively, and a is the activity of the species.

For carbonate minerals, dissolution/precipitation mechanisms are catalyzed by HCO₃⁻, and reaction rates depend on the activity of aqueous CO₂. k_n is calculated according to:

$$k_n = k_{25}^{nu} \exp\left[\frac{-E_a^{nu}}{R}\left(\frac{1}{T} - \frac{1}{298.15}\right)\right] + k_{25}^H \exp\left[\frac{-E_a^H}{R}\left(\frac{1}{T} - \frac{1}{298.15}\right)\right] a_H^{n_H} + k_{25}^{CO_2} \exp\left[\frac{-E_a^{CO_2}}{R}\left(\frac{1}{T} - \frac{1}{298.15}\right)\right] a_{CO_2}^{n_{CO_2}}$$

The kinetic parameters used for the last two equations are from Palandri and Kharaka (2004).

Mineral dissolution and precipitation reactions involve temporal changes in reservoir porosity. Indeed, variations in the mineral volume fraction owing to chemical reactions allow computing the resulting porosity. Permeability variations are calculated from porosity changes using the "tube-in-series" model (Verma and Pruess, 1988), which allows reaching nil permeability even if porosity is not nil.

Geometrical Model

The saline aquifer is schematically represented by a 2D-radial model including the reservoir and caprock units (Figure 1).

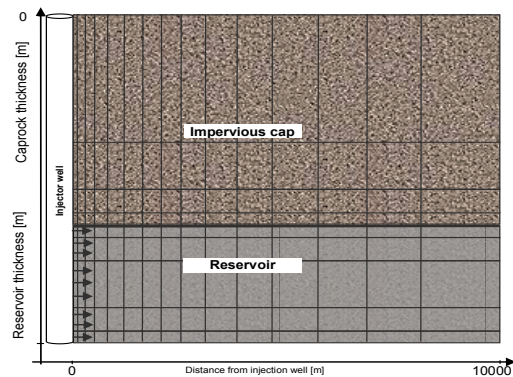


Figure 1. Scheme of the geometrical 2-D radial model (vertical cross-section).

This conceptual model is able to evaluate the evolution of the geochemical reactivity induced by gas injection, both in time and in space. The 200 m thick reservoir is centered on a vertical injection well with a radius of 0.2 m. Maximum radial extent is 100 km. The investigated system is represented by 800 gridblocks comprising the model mesh. Along the radius axis, 29 grid cells are considered between 0.2 m and 1 km, 50 grid cells between 1 km and 10 km, and 20 grid cells between 10 and 100 km. In each interval, the width of the radial elements follows a logarithmic scale. Vertical discretization is achieved by dividing the reservoir into 5 layers (from bottom to top, 20, 40, 80, 40, and 20 m), and the caprock into 3 layers (5, 10, and 25 m).

Reservoir Characteristics

The investigated saline aquifer is a sandstone reservoir of about 200 m thickness. The effective pressure and temperature before any injection are 150 bar and 50°C, respectively.

Since the reservoir rock's porosity ranges between 13 and 18%, an average value of 15% is selected for the calculations. The porosity of the caprock is estimated to be 40%.

The caprock level presents a mean permeability of 0.003 mD, whereas the permeability of the saline reservoir is about 300 mD.

Due to the injection of a gas phase within the deep system, the relative permeability and the capillary pressure characteristics of the medium must be defined to accurately describe the relative flow of gas with respect to the aqueous solution. Since we lacked petrophysical data for the targeted reservoir, we conducted a bibliographic review to define the representative curves and to implement them into the numerical code. Bachu and Bennion (2007) listed data concerning sandstones. Owing to the characteristics of the investigated reservoir ($k_{\text{mean}} \# 300 \text{ mD}$; $\Phi \# 15\%$; $P_{\text{reservoir}} = 150 \text{ bars}$; $T = 50^\circ\text{C}$), we found an analogy with the Cardium sandstone and chose it as the reference sandstone (Figure 2). The same characteristic curves for relative permeability and capillary pressure are used for the reservoir and the caprock layer.

For the numerical simulations, the minerals present in the caprock and in the reservoir are

selected in conjunction with the mineralogical assemblage determined from core analysis. But some adjustments were made, according to the database used by TOUGHREACT.

The caprock is essentially composed of illite and quartz (77 wt%) while the reservoir rock essentially contains quartz and K-feldspar (91 wt%). Since a plagioclases series (solid solution) is not included in the database, the end-member albite ($\text{NaAlSi}_3\text{O}_8$) was chosen as a substitute.

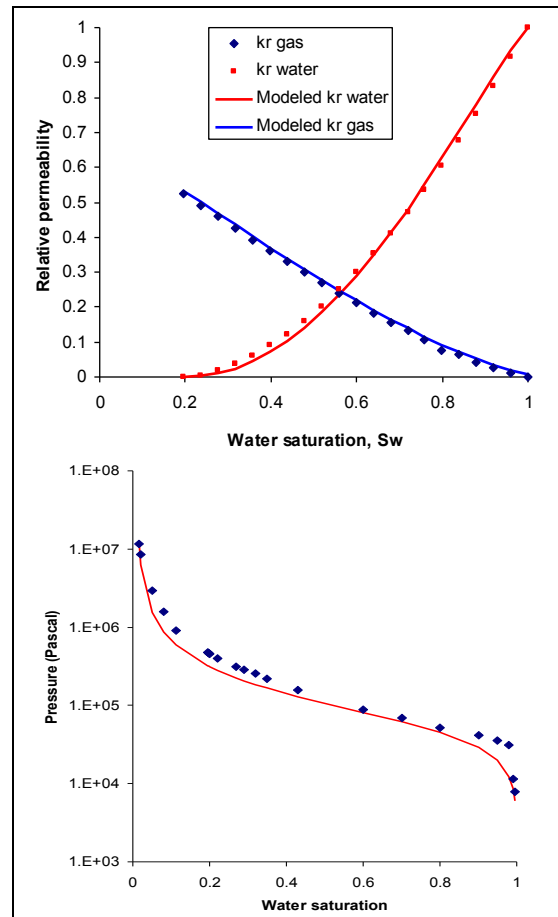


Figure 2. Relative permeability (upper figure) and capillary pressure (lower figure) curves for Cardium sandstone (symbols are from Bennion and Bachu, 2005). Fitted curves are implemented in TOUGHREACT code.

Chlorite (chloritoid series) is not in the database, so the clinocllore-7A ($\text{Mg}_5\text{Al}_2\text{Si}_3\text{O}_{10}(\text{OH})_8$) was chosen as a chlorite analogue (Gaus et al., 2005). Magnesite (MgCO_3) is used instead of siderite (FeCO_3), as it is more stable in the initial system at thermodynamic equilibrium. This substitution is acceptable, since magnesite is also a carbonate

that acts as a pH buffer as well as siderite. Rutile and anatase are common detrital minerals. Anatase, which comes from Ti-bearing minerals, is chosen for this study (Table 1).

Table 1. Selected mineralogical composition of the caprock and the reservoir rocks.

	Minerals	Wt%
Caprock	Illite	60
	Quartz	17
	Albite	6
	Clinocllore-7A	5
	K-Feldspar	4
	Hematite	4
	Magnesite	3
	Anatase	1
Reservoir	Quartz	81
	K-Feldspar	10
	Albite	5
	Calcite	3.6
	Anhydrite	0.4

Chemical composition of water

Detailed physico-chemical characteristics of the formation water are provided in Table 2. The chemical analyses are performed in the laboratory at ambient conditions (1 bar, 25°C).

Table 2. Chemical composition of the aquifer water.

Element	Concentration (mg L ⁻¹)
Na (as Na ⁺)	90283
K (as K ⁺)	624
Ca (as Ca ²⁺)	13652
Mg (as Mg ²⁺)	2206
N (as NH ₄ ⁺)	11
Fe (as Fe ²⁺)	127
Cl (as Cl)	171449
Br (as Br)	1162
I (as I)	7.4
S (as SO ₄ ²⁻)	566.2
Total Dissolved Salt	280 000

The water composition for *in situ* conditions (150 bars, 50°C) is evaluated based on some relevant hypothesis and the thermodynamic calculations relevant for highly saline aqueous systems using the SCALE2000 code (Azaroual et al., 2004). The pH and bicarbonate concentration of this brine are recalculated for the reservoir pressure and temperature conditions, assuming that the brine is in thermodynamic equilibrium with respect to calcite. This resulted in a bicarbonate concentration of 103 mg L⁻¹. Under these

conditions, the brine remains slightly undersaturated with respect to the evaporitic minerals (halite, sylvite and anhydrite), but is slightly supersaturated with respect to dolomite and pyrrhotite (iron sulfide).

NUMERICAL SIMULATIONS

Initial Conditions and Injection Procedure

The assumptions for numerical modeling are as follows:

➤ *Hydrostatic equilibrium*: no regional flow is considered, and a hydrostatic pressure is imposed in the outermost column of the mesh.

➤ *Thermal equilibrium*: before starting gas injection, reservoir and caprock are at the same temperature, i.e., 50°C. The numerical simulations are performed in isothermal mode.

➤ *Geochemical equilibrium*: the aqueous solutions initially present within the reservoir and caprock are in equilibrium with their respective mineral assemblages at the temperature of the system.

➤ *Injection rates of supercritical CO₂ and SO₂-O₂ dissolved in brine*: these are respectively 30 kg s⁻¹ and 15 kg s⁻¹. The mass ratio of 2 has been arbitrary chosen for these simulations. Gas and brine are injected over the total thickness of the reservoir during an assumed exploitation period of 30 years.

A mixture of supercritical CO₂ and reservoir brine containing SO₂ and O₂ (namely “SO₂-O₂ brine”) are co-injected into the reservoir, because the TOUGHREACT does not handle CO₂-SO₂-O₂-H₂O gas mixtures, only CO₂-H₂O mixtures (specificity of the ECO2n module). Two gas streams mixtures are investigated:

➤ “Low SO₂-O₂ brine” containing CO₂ (91.61 vol%) and 9.71 vol% of impurities, including a negligible SO₂ (0.08 vol%) and 1.6 vol% of O₂.

➤ “High SO₂-O₂ brine” containing 90.28 vol% of CO₂, 1.53 vol% of SO₂, and 1.6 vol% of O₂.

The chemical composition of the SO₂-O₂-acidified brine is handled in different steps:

➤ The injected brine is first equilibrated with the minerals of the reservoir.

➤ SO₂ and O₂ gases are then dissolved within the brine. Given the chosen mass ratio of 2 between the injected mass of supercritical CO₂

and the mass of SO₂-O₂ brine, the SO₂ and O₂ concentrations within the solution are defined to ensure consistency with the gas composition of an oxy-combustion capture process (given by data from the industry). Such preliminary simulations are performed with the batch option of the PHREEQC code (Parkhurst and Appelo, 1992). The hypothesis that SO₂ is fully dissolved within the SO₂-O₂ brine is acceptable, since its solubility is very high at such temperatures.

➤ The activity model used in the batch simulations is the Davies model. The TOUGHREACT code uses an extended Debye-Hückel model, although admittedly those models are not adapted for highly saline solutions such as in the targeted reservoir (Table 2). For this reason, and for more reliable results, the elemental concentrations of each species of the acidified water are divided by a factor of 10, in order to decrease the ionic strength of the solution (Table 3). This artificial dilution does not drastically modify the simulation results (e.g., reaction paths, dissolution/precipitation magnitudes of minerals) even if it significantly changes the initial saturation state of waters with respect to rock minerals.

Table 3. Chemical characteristics of the fluids used for numerical calculations.

	Reservoir brine	Low SO ₂ -O ₂ brine	High SO ₂ -O ₂ brine
pH	7.9	1.5	0.2
pe	-3.9	17.7	19.0
TDS (g/kg _{H2O})	38.6	~38.6	~38.6
[SO ₄ ⁻²](mol/L)	1.7e-02	5.0e-02	7.2e-01

The “SO₂-O₂ brines” are very acid, with oxidative and sulfate concentrations higher than in the reservoir brines. These brines are expected to be highly reactive with reservoir minerals.

Results

Case 1: Injection of “a low SO₂-O₂ brine”

The gas and water injection within the reservoir drive changes of physical parameters (gas saturation, pressure, and so forth) and geochemical properties at different scales, with a major impact on the near-wellbore zone.

First, due to the injection of the gas/solution mixture, the gas saturation changes around the injection well. Because the supercritical CO₂

density is lower than that of the formation brine, CO₂ reaches preferentially the top of the aquifer and expands along it (Figure 3). The caprock is less permeable than the reservoir, but considering the selected permeability, the supercritical CO₂ can penetrate it to a certain extent. The pressure around the injector increases to reach 167 bars during the injection period. (Initially, the pressure ranged between 143 and 160 bars between the top and the bottom of the reservoir.)

The pH of the formation water is controlled by water-rock interactions. Initially, the formation water is in equilibrium with the mineral assemblage of the reservoir: the pH is close to 7.9 (Table 3). Co-injection of supercritical CO₂ and SO₂-O₂ brine then modifies this equilibrium: the evolution of pH follows the evolution of the gas saturation within the reservoir, with the impacted zone extending up to 3000 m from the injector after an injection period of 30 years (Figure 3). Consequently, the formation water around the injector acidifies, becomes under-saturated with respect to all minerals, and dissolves them (preferentially the carbonates). As long as reactive carbonates are present, the aqueous solution is in equilibrium with them and the pH is buffered. However, with extended injection, some minerals are exhausted: all carbonates are consumed around the injector and the buffering effect stops. pH is not controlled and decreases to very low values. Near the well, the mineral assemblage is drastically modified, and the pH decreases to a minimum value of 1.4, close to the value of the injected fluid (Table 3). Further within the impacted zone of the reservoir, the pH is buffered to a value ranging between 4 and 6, since not all the carbonates are consumed. The pH is unchanged in the non-impacted zone.

Calcite is the mineral most affected by injection of the acid solution; it dissolves near the injection well (50 m around it), but it is little impacted elsewhere in the reservoir (Figure 3). The other mineral affected by gas and water injection is anhydrite. The behavior of anhydrite differs in time and space: at first, anhydrite precipitates near the injection well, because the injected fluid contains sulfur, oxidized to sulfate by oxygen. Calcite is dissolved by the acidified injected water, releasing Ca²⁺ in solution. With

SO_4^{2-} present in the injected water, these ions combine to form anhydrite.

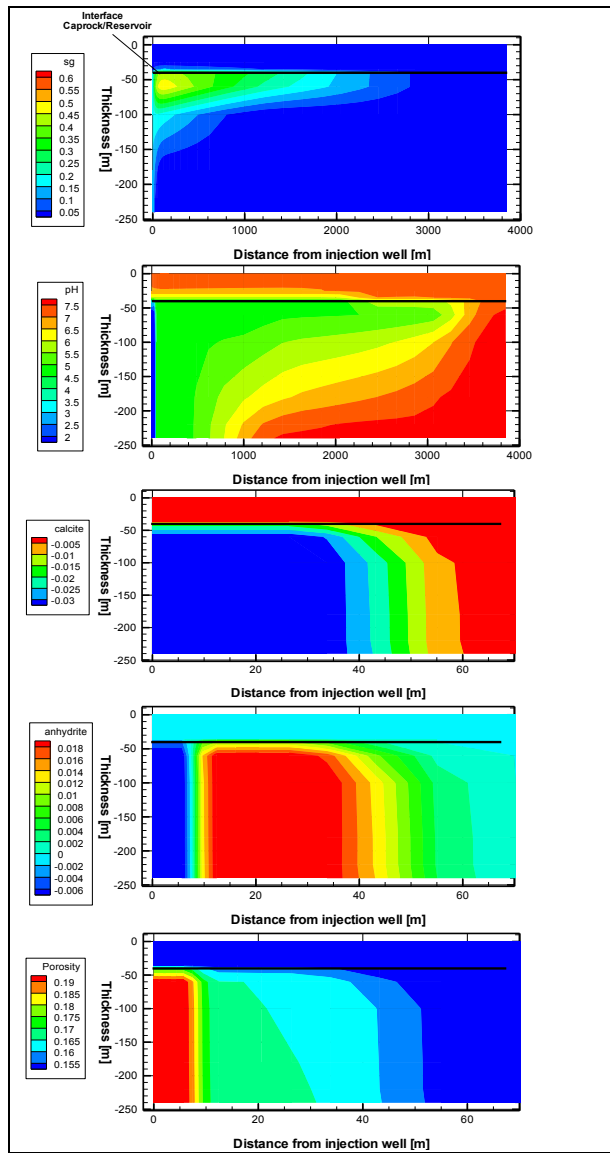


Figure 3. State of the reservoir and caprock after an injection period of 30 years. From top to bottom: gas saturation (Sg), pH with x-axis up to 4000 m, volumic fraction of calcite, volumic fraction of anhydrite and porosity with x-axis up to 400 m.

However, when all the calcite is consumed, the Ca^{2+} source disappears, and anhydrite precipitation stops. Because the injected solution is undersaturated with respect to anhydrite, the secondary precipitated anhydrite and the original anhydrite (initially present within reservoir) dissolve. This is why some zones present a deficit of anhydrite, whereas others present a

positive balance of anhydrite compared to its initial amount (Figure 3).

As a consequence of calcite and anhydrite reactivity, porosity increases near the injector (Figure 3). After an injection period of 30 years, at 10 m from the injection well, a porosity of about 19% is estimated (due to calcite and anhydrite dissolution). This value is probably overestimated: in a real injection, a CO_2/SO_2 gas mixture would be injected, preventing the dissolution of primary and secondary anhydrite. Consequently, if anhydrite did not dissolve, the expected porosity would range between 16.5 and 17% (values deduced from the porosity variations between 10 and 40 m from injector). In any case, these values need to be considered as indicative (qualitative) and not effectively quantitative, because of some limiting working hypotheses (dilution of the initial brine, limitations of kinetic parameters, etc.).

All other minerals react but in fewer proportions than calcite and anhydrite (2 to 5 orders of magnitude lower), and their impact on porosity is negligible. Because of the assumptions made regarding caprock permeability, supercritical CO_2 is able to slightly penetrate within it. But the CO_2 amounts are too low and the impact on chemical reactivity and porosity variations are too limited to be seen in the graphical representations of the numerical simulations. Moreover, additional data are needed to better define the hydraulic properties of the caprock and improve the quality of these simulations.

Case 2: Injection of a “high $\text{SO}_2\text{-O}_2$ brine”

The same simulation as in the case 1 was performed. At the temperature of the reservoir (i.e. 50°C), the “high- SO_2 brine” is slightly over-saturated with respect to anhydrite. Consequently, after an injection period of 12 years, the anhydrite precipitation fully clogs the porosity around the injection well, indicating the end of the injection if no measures were taken to keep the injectivity stable.

To analyze anhydrite precipitation conditions, we conducted another simulation with a new injected solution. In this last case, the original reservoir brine, still 10-times diluted, was not initially equilibrated with the mineralogical assemblage of the reservoir before adding SO_2

and O₂. In this case, the injected solution was undersaturated with respect to anhydrite.

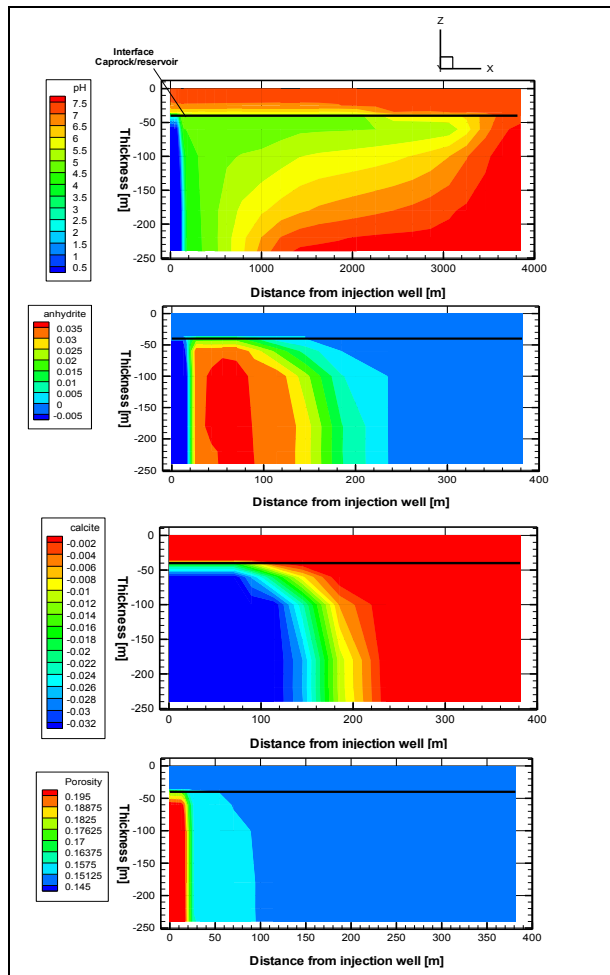


Figure 4. State of the reservoir and caprock after an injection period of 30 years. From top to bottom: pH with x-axis up to 4000 m, volumic fraction of anhydrite, volumic fraction of calcite and porosity with x-axis up to 400 m.

The resulting impact of the co-injection of supercritical CO₂ and acidified brine is a decrease in pH around the injection well and a co-dissolution of both carbonates and anhydrite (since the solution is under-saturated with respect to anhydrite) (Figure 4). Since the acidity is higher than for the “low SO₂-O₂ brine” (Table 3), the impacted zone is also more extended than in the first case (about 50 m in case 1 compared to 200 m in case 2).

The other minerals of the assemblage were also impacted by this strong acidification. They were relatively less impacted than carbonates or anhydrite, but the dissolution of some of them

(K-feldspar) and precipitation of others (quartz, kaolinite) must be carefully tracked.

In this last case, the higher acidity of the injected fluid is neutralized to a lesser extent by reactions with minerals: less important variations in porosity are observed in the near-well domain, whereas the impacted zone is extended by the dissolution and precipitation reactions.

CONCLUSIONS

The objectives of this paper were to present the results from numerical simulations of the co-injection of acid gases within a deep saline aquifer. Since the TOUGHREACT code cannot represent the co-injection of these components in a gaseous (nonwetting phase) mixture, some limiting hypotheses were done: CO₂ injection was simulated as in a supercritical form, whereas SO₂ and O₂ injections were simulated as in dissolved species within an aqueous solution. After an injection period of 30 years, simulation results indicate:

- The injected supercritical CO₂ dissolves in solution, increasing its ability to dissolve carbonates. Since calcite is one of the components of the mineralogical assemblage, it dissolves around the injection well and therewith increases porosity. But because of the negligible calcite in the mineralogical assemblage, the impact on pore volume is quite limited.
- SO₂ reacts rapidly around the injection well, forming sulfates because of the traces of oxygen in the injected gas. Through the recombining of Ca²⁺ (coming from calcite) and SO₄²⁻ (issued from SO₂ and O₂), anhydrite precipitates. The SO₂ concentration (low or high) determines the extent of the anhydrite deposition occurring in a radius around the injection well.
- The higher the SO₂ concentration in the injected stream, the larger the radius of anhydrite deposition around the well. However, the SO₂ concentration seems to have no influence on the geochemical mechanisms in terms of (for instance) reaction paths.
- Calcite and anhydrite are the most reactive minerals. All the other initial minerals are also affected by the injection of acid solution, but in less proportion and with a minor impact on porosity and permeability.

➤ When calcite and anhydrite present opposite behaviors, numerical simulations forecast that calcite dissolution will have a more important impact on porosity than anhydrite precipitation. Consequently, increasing porosity is expected around the injection well, supposing an increase in well injectivity and a potential long-term injection period.

However, we must consider these results as qualitative, highlighting only the global trends of the investigated system. Indeed, the real impact (quantitative estimation) is still very difficult to predict. For example, how the dissolution/precipitation of a particular mineral will affect rock porosity will depend on the characteristics of the rock (e.g., micro/macroporosity, connected porosity). Thus, our results must be interpreted cautiously.

ACKNOWLEDGMENT

This work is part of the OXYGAS (phase II) project funded by VATTENFALL. The authors acknowledge the VATTENFALL Directorate and BRGM Research Directorate for allowing publication of these results at the Symposium.

REFERENCES

André L., P. Audigane, M. Azaroual, and A. Menjoz, Numerical modeling of fluid-rock chemical interactions at the supercritical CO₂-liquid interface during supercritical carbon dioxide injection into a carbonated reservoir, the Dogger aquifer (Paris Basin, France). *Energ. Conv. Manage.*, 48, 1782-1797, 2007.

André L., M. Azaroual, and A. Menjoz, Numerical Simulations of the Thermal Impact of Supercritical CO₂ Injection on Chemical Reactivity in a Carbonate Saline Reservoir. *Transp. Porous Med.*, 82, 247-274, 2010.

Azaroual M., C. Kervévan, P. Durst, and M.-V. Durance, SCALE2000 (V3.1) : Logiciel de calculs thermodynamiques et cinétiques ; application aux saumures pétrolières, hydrothermales et industrielles. Manuel d'utilisation; BRGM Editions, ISBN2-7159-0939-X. 70 p., 2004.

Bachu S., and B. Bennion, Effects of in-situ conditions on relative permeability characteristics of CO₂-brine systems,

Environ. Geol., 54, 1707–1722, 2007.

Bennion B., and S. Bachu, Relative permeability characteristics for CO₂ displacing water in a variety of potential sequestration zones in the Western Canada Sedimentary Basin. *SPE Paper 95547*, 15 p., 2005.

Gaus I., M. Azaroual, and I. Czernichowski-Lauriol, Reactive transport modelling of the impact of CO₂ injection on the clayey caprock at Sleipner (North Sea). *Chem. Geol.*, 217, 319-337, 2005.

Lasaga A.C., Chemical kinetics of water-rock interactions, *J. Geophys. Res.*, 89, 4009-4025, 1984.

Palandri J., and Y.K. Kharaka, A compilation of rate parameters of water-mineral interaction kinetics for application to geochemical modelling. *US Geol. Surv. Open File Report 2004-1068*, 64 p., 2004.

Parkhurst D.L., and C.A.J. Appelo, User's guide to PHREEQC (Version 2) - A computer program for speciation, batch-reaction, one-dimensional transport, and inverse geochemical calculations. *Water-Resources Investigations Report 99-4259*, US Geol. Surv., 1999.

Pruess K., C.M. Oldenburg, and G.J. Moridis, TOUGH2 User's Guide, Version 2.0. Lawrence Berkeley National Laboratory Report LBNL-43134, Berkeley, CA (USA), 1999.

Pruess K., ECO2n: a TOUGH2 fluid property module for mixtures of water, NaCl and CO₂. Lawrence Berkeley National Laboratory Report LBNL-57952, Berkeley, CA (USA), 2005.

Verma A., and K. Pruess, Thermohydrologic conditions and silica redistribution near high-level nuclear wastes emplaced in saturated geological formations, *J. Geophys. Res.*, 93(B2), 1159–1173, 1988.

Wolery T., EQ3/6: Software package for geochemical modeling of aqueous systems: Package overview and installation guide (version 7.0). Report UCRL-MA-210662, Lawrence Livermore National Laboratory, CA (USA), 1992.

Xu T., and K. Pruess, Modeling multiphase non-isothermal fluid flow and reactive geochemical transport in variably saturated fractured rocks: 1. Methodology, *Am. J. Sci.*, 301, 16-33, 2001.